

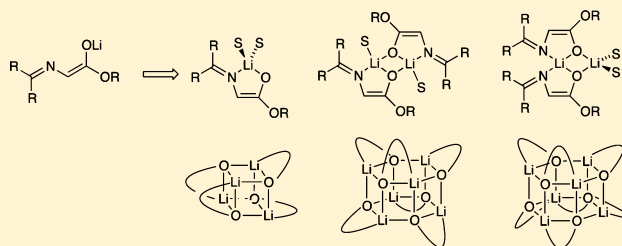
# Solid-State and Solution Structures of Glycinimine-Derived Lithium Enolates

Kyoung Joo Jin and David B. Collum\*

Department of Chemistry and Chemical Biology, Baker Laboratory, Cornell University, Ithaca, New York 14853-1301, United States

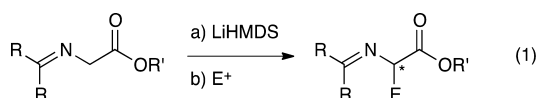
**S** Supporting Information

**ABSTRACT:** A combination of crystallographic, spectroscopic, and computational studies was applied to study the structures of lithium enolates derived from glycinimines of benzophenone and (+)-camphor. The solvents examined included toluene and toluene containing various concentrations of tetrahydrofuran, *N,N,N',N'*-tetramethylethylenediamine (TMEDA), (*R,R*)-*N,N,N',N'*-tetramethylcyclohexanediamine [(*R,R*)-TMCDA], and (*S,S*)-*N,N,N',N'*-tetramethylcyclohexanediamine [(*S,S*)-TMCDA]. Crystal structures show chelated monomers, symmetric disolvated dimers,  $S_4$ -symmetric tetramers, and both  $S_6$ - and  $D_{3d}$ -symmetric hexamers.  $^6\text{Li}$  NMR spectroscopic studies in conjunction with the method of continuous variations show how these species distribute in solution. Density functional theory computations offer insights into experimentally elusive details.



## INTRODUCTION

Glycinimines have been used as synthons in the preparation of amino acid derivatives from glycine (eq 1).<sup>1–4</sup> Benzo-



phenone-based imine **1** has received considerable attention in the context of phase-transfer-catalyzed alkylations.<sup>2</sup> Alkylations of the corresponding lithium enolates of camphor-derivative **3** have been examined, although the yields and selectivities are variable.<sup>3,4</sup> Lithiated glycinimines captured our imagination as possible targets for studies of the effects of aggregation and solvation on reactivity and stereoselectivity.<sup>5</sup>

Herein we describe X-ray crystallographic, NMR spectroscopic, and density functional theory (DFT) computational studies of glycinimine enolates **1–3** ( $R = \text{Me}, \text{Et}, \text{tert-Bu}$ ) solvated by several mono- and bidentate ligands. These studies reveal diverse structural motifs, including those of monomer **4**, symmetric and unsymmetric (spirocyclic) dimers **5** and **6**,  $S_4$ -symmetric tetramer **7**,  $S_6$ -symmetric hexamer **8**, and  $D_{3d}$ -symmetric hexamer **9** (Chart 1). The spectroscopic studies reveal solvent-dependent aggregate distributions in solution.<sup>6</sup>

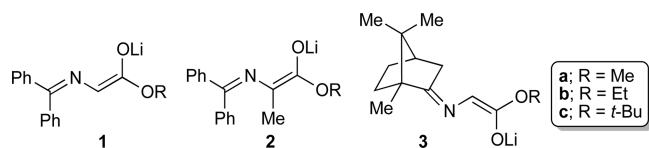
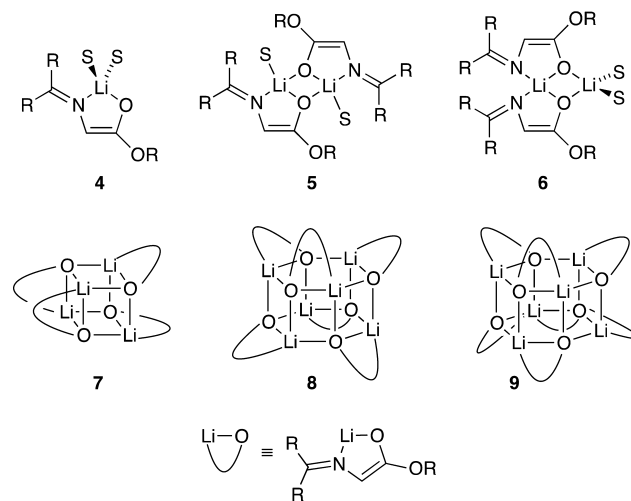


## Chart 1



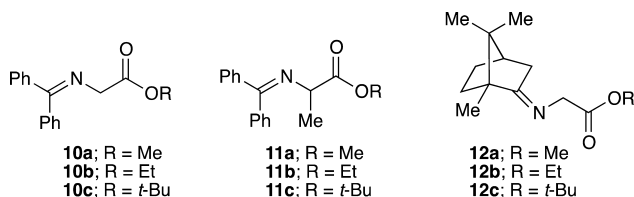
## RESULTS

**Substrates.** Glycinimines **10–12** were prepared by condensing glycine esters with benzophenone or thiocamphor via literature protocols.<sup>3a,h</sup> Enolates **1–3** were prepared in situ from glycinimines **10–12** with the solvent(s) of choice from recrystallized lithium hexamethyldisilazide ( $^6\text{Li}$ )LiHMDS or  $^6\text{Li}, ^{15}\text{N}$ LiHMDS.<sup>7</sup> Slow aggregate equilibration demanded aging at 25 °C for  $\geq 60$  min before spectroscopic analysis. Although we focus on the methyl esters **1a** and **3a**, crystallinity or

Received: September 9, 2015

Published: November 10, 2015

superior spectroscopic behaviors occasionally bring the ethyl and *tert*-butyl esters as well as the alanine derivative **2a** into play. The Supporting Information archives key experimental data and results that are not mentioned herein. We begin with a survey of crystal structures.



**X-ray Crystal Structure: Monomer 4c.** The addition of 1.10 equiv of LiHMDS (0.11 M in toluene) to a solution of glycinimine **10c** generated a 0.10 M solution of enolate **1c** in toluene with 0.50 M *N,N,N',N'*-tetramethylethylenediamine (TMEDA) at  $-78$  °C. After the solution was warmed to 25 °C, pale yellow crystals formed overnight, and their composition as TMEDA-chelated monomer **4** was confirmed with X-ray diffraction (Figure 1). Enolate **1c** crystallizes in the monoclinic

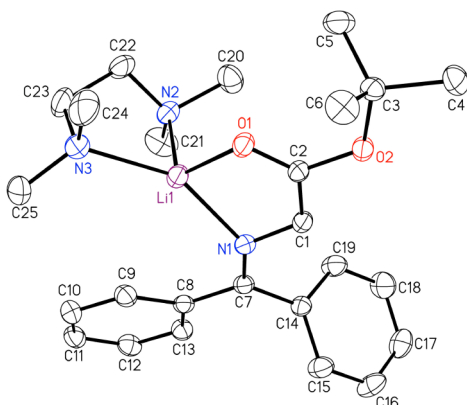


**Figure 1.** X-ray crystal structure of *N,N,N',N'*-tetramethylethylenediamine (TMEDA)-chelated monomer **4c** derived from enolate **1c**.

$P2(1)/n$  space group. Monomer **4c** displays a chelating TMEDA ligand and an N,O-chelate of the substrate that is common to all crystallographically determined glycinimine enolates.

**X-ray Crystal Structure: Symmetric Dimers 5b.** The crystallization of enolate **1b** (0.20 M) from pentane containing TMEDA (4.45 M) at  $-20$  °C afforded dimer **5b** bearing two  $\eta^1$ -coordinated TMEDA ligands disposed antarafacially to each other (Figure 2) in the triclinic space group  $P1$ . Monodentate TMEDA ligands have been detected crystallographically, spectroscopically, and kinetically.<sup>8,9</sup> Enolate **1b** was crystallized from a 0.10 M enolate solution in neat tetrahydrofuran (THF) at 25 °C to afford THF-solvated dimer **5b** (Figure 3), which is structurally similar to the TMEDA-solvated **5b**.

**X-ray Crystal Structure: Tetramer 7a.** A 0.10 M solution of benzophenone-derived enolate **2a** in 6.40 M Et<sub>2</sub>O/toluene deposited pale yellow crystals after standing at 25 °C for 3 days. X-ray diffraction analysis (Figure 4) shows tetramer **7a** in the monoclinic space group  $C2/c$ . The alternating N,O-chelated enolates correspond to an  $S_4$ -symmetric cubic core (7).

**X-ray Crystal Structure: Hexamer 8b.** A 0.10 M solution of benzophenone-derived enolate **1b** in toluene was prepared at  $-78$  °C. The solution was warmed to 25 °C and yielded pale yellow crystals overnight. X-ray diffraction analysis (Figure 5)

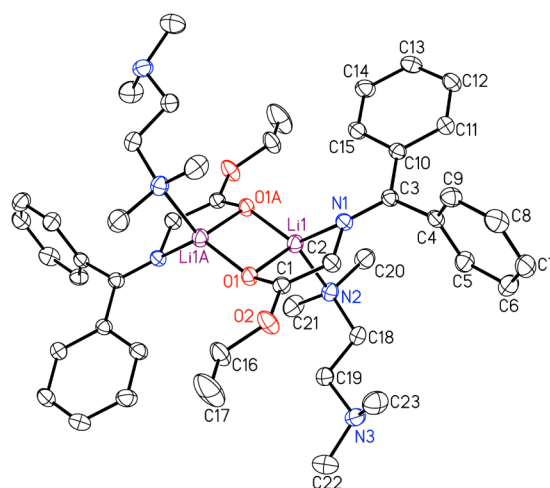


**Figure 2.** X-ray crystal structure of  $\eta^1$ -TMEDA-solvated dimer **5b** derived from enolate **1b**.

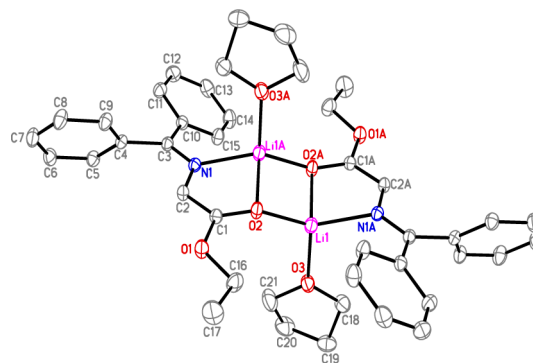


**Figure 3.** X-ray crystal structure of tetrahydrofuran (THF)-solvated dimer **5b** derived from enolate **1b**.

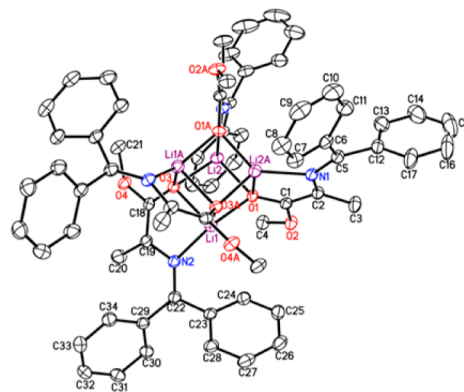


**Figure 4.** X-ray crystal structure of unsolvated  $S_4$ -symmetric tetramer **7a** derived from enolate **2a**.

shows that complex **8b** crystallizes in the monoclinic space group  $P2(1)/n$  as a hexamer. The alternating N,O-chelated enolates on a hexagonal drum afford an  $S_6$ -symmetric core. Apparent ethoxy–lithium contacts may be stabilizing.

**X-ray Crystal Structure: Hexamer 9a.** A 0.10 M solution of camphor-derived enolate **3a** in 1:2 tetramethylsilane<sup>10</sup>/pentane afforded colorless crystals after standing at  $-20$  °C for 2 days. X-ray diffraction analysis (Figure 6) shows hexamer **9a** in the monoclinic space group  $P2(1)$ . The N,O-chelated enolates correspond to a  $D_{3d}$ -symmetric cubic core.

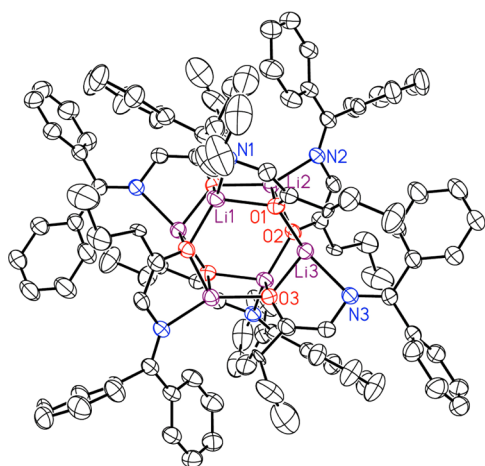


**Figure 5.** X-ray crystal structure of unsolvated  $S_6$ -symmetric hexamer **8b** derived from enolate **1b**.

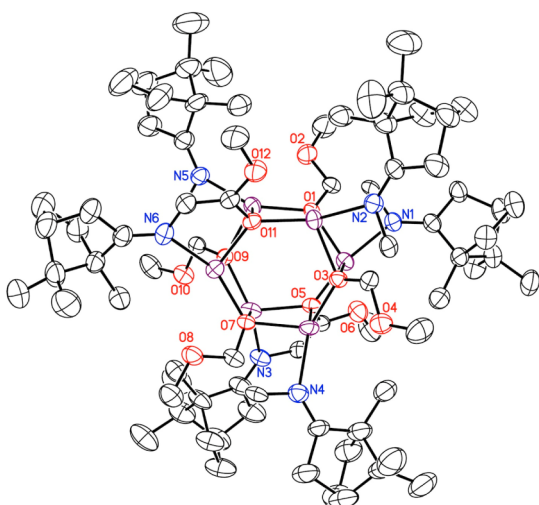
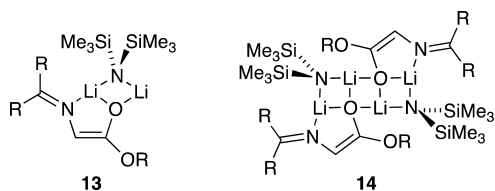


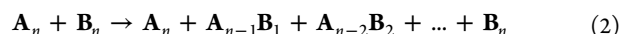
**Figure 6.** X-ray crystal structure of unsolvated  $D_{3d}$ -symmetric hexamer **9a** derived from enolate **3a**.

**Solution Structures: General Protocols.** The enolates were characterized in solution with a series of techniques centering on  $^6\text{Li}$  NMR spectroscopy. Standard  $^6\text{Li}$  spectra were recorded as a function of enolate and donor ligand concentrations to assess relative aggregation and solvation states.  $^{15}\text{N}$ -labeled glycinimine enolates confirmed the presence of chelation.  $[\text{}^6\text{Li},^{15}\text{N}]\text{LiHMDS}$  was used to exclude mixed aggregation in the presence of donor ligands.<sup>11</sup> However, enolate **1a** or **3a** with excess  $[\text{}^6\text{Li},^{15}\text{N}]\text{LiHMDS}$  in neat toluene afford, in addition to the homoaggregates discussed below, two  $^6\text{Li}$  doublets consistent with substructure **13** likely derived from ladder **14**.<sup>12,13</sup>



Although the crystal structures are helpful, a critical arbiter of solution structure stems from the method of continuous variations (MCV).<sup>14,15</sup> In short, MCV overcomes the problems

of high homoaggregate symmetry,  $A_n$  and  $B_n$ , by generating an ensemble of homo- and heteroaggregates (eq 2). The number of heteroaggregates, their dependence on subunit mole fraction ( $\chi_A$  or  $\chi_B$ ), and their spectroscopically detected symmetries provide the aggregation state,  $n$ . In higher aggregates, especially hexamers, positional isomerism and the stereochemistry of chelation cause inordinate complexity.<sup>15c</sup> Warming the sample to elicit chelate exchange and intra-aggregate lithium–lithium site exchange<sup>16</sup> symmetrizes the heteroaggregates, which causes each  $A_nB_n$  stoichiometry to appear as a single  $^6\text{Li}$  resonance.<sup>14</sup> A graph of concentration versus mole fraction affords a Job plot<sup>17</sup> (exemplified by Figure 9) in which a parametric fit reveals minimal deviations from statistical distributions.



The presence or absence of solvation can be inferred from solvent-dependent chemical shifts. A particularly useful trick is to add increments of pyridine, which shifts resonances corresponding to solvated  $^6\text{Li}$  nuclei markedly downfield and leaves unsolvated resonances unchanged.<sup>18</sup>

Some comments about structural variations are warranted. MCV analyses rely on binary combinations of methyl, ethyl, and *tert*-butyl ester enolates with distinctly different chemical shifts to form  $A_n$ – $B_n$  ensembles with optimal resolution. In many instances, different esters afford alternative views of similar structures; we typically focus on the ester offering optimal resolution. In some instances, however, variations are merely historical owing to the chronology of the exploration. When it is clarifying, an explanation is given for the choice of substrate.

**Solution Structures: Toluene.** After aging at 25 °C in toluene, benzophenone-derived enolate **1a** affords two homoaggregates (Figure 7) shown to be a hexamer and a tetramer. The

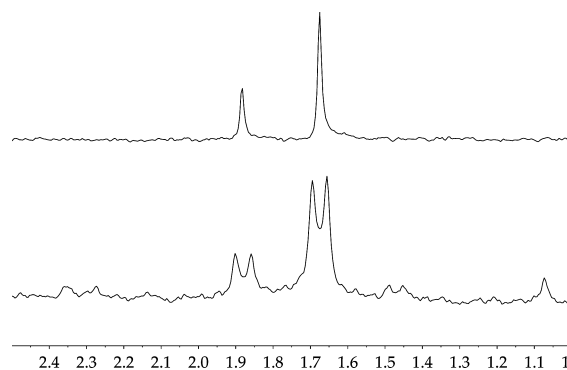


**Figure 7.**  $^6\text{Li}$  NMR spectra of 0.10 M  $[\text{}^6\text{Li}]\mathbf{1a}$  (top) and  $[\text{}^6\text{Li},^{15}\text{N}]\mathbf{1a}$  (bottom) in toluene at  $-70$  °C.

downfield resonance at 1.88 ppm increases with concentration, which indicates that it is the larger of the two. Each resonance of  $[\text{}^6\text{Li},^{15}\text{N}]\mathbf{1a}$  was a doublet ( $J = 3.0$  Hz), which confirms that both are chelated and that chelate exchanges are slow. The consequences of rapid chelate exchange on resonance counts, multiplicities, and coupling constants are discussed below. The major and minor resonances coalesce to a single resonance above  $-10$  °C.

To apply MCV, we turned to camphor-derived enolate **3a**, which displays a single resonance at high concentrations with a minor shoulder (corresponding to the lower aggregate) emerging on dilution. Under conditions in which the two higher homoaggregates dominate, mixtures of **1a** and **3a** in toluene

generate complex spectra at low temperatures. This complexity arises from positional isomerism<sup>15c</sup> within the heteroaggregates. Warming to 35 °C, however, imparts rapid intra-aggregate lithium–lithium site exchanges<sup>16</sup> and chelated exchanges that reveal clean ensembles with seven resonances consistent with hexamers (Figure 8). (Interaggregate exchange at much higher

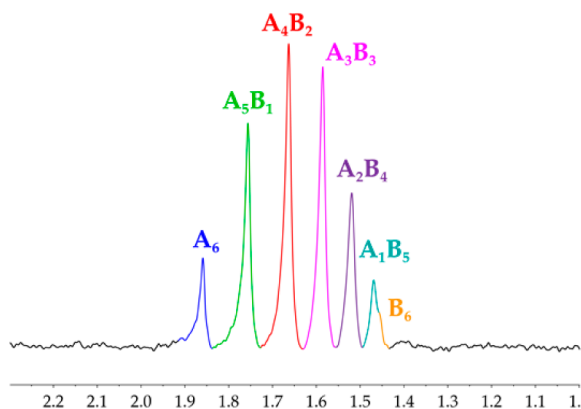


**Figure 8.** <sup>6</sup>Li NMR spectrum of a 1:1 mixture of **1a** ( $A_6$ ) and **3a** ( $B_6$ ) in toluene at 35 °C and a 0.10 M total enolate concentration showing an ensemble of homo- and heteroaggregates as labeled.

temperatures would average all resonances to a single resonance and, in the case of labeled species, cause loss of <sup>6</sup>Li–<sup>15</sup>N coupling.) Monitoring the ensemble as a function of mole fraction affords the Job plot in Figure 9.

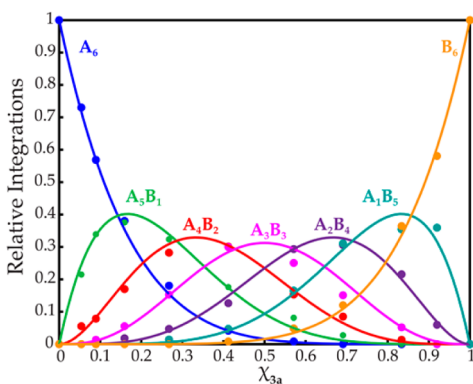
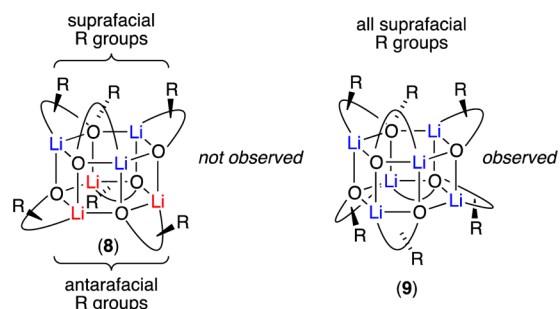


**Figure 9.** Job plot showing the relative integrations of hexameric homo- and heteroaggregates versus measured<sup>19</sup>F mole fractions of **3a** ( $\chi_{3a}$ ) from mixtures of **1a** and **3a** (0.10 M total enolate concentration) at 35 °C (see Figure 8).

Two hexameric topologies were detected crystallographically:  $S_6$ -symmetric hexamer **8b** was observed for enolate **1b** (Figure 5), and  $D_{3d}$ -symmetric hexamer **9a** derived from enolate **3a** (Figure 6). Therefore, we are forced to rely on crystallographic analogy and computations (below) to complete the assignments (*vide infra*). We note, however, that  $S_6$ -topology in **8a** derived from chiral enolate **3a** should afford a doubling of the <sup>6</sup>Li resonance; the lithiums around the top and bottom hexagons are not magnetically equivalent.<sup>15</sup> No such doubling was observed. Thus, the solution structure of the hexamer derived from enolate **3a** appears to be the  $D_{3d}$  form **9a** found crystallographically (Figure 6).

The observable minor aggregates of enolates **1a** and **3a** were assigned as tetramers. The absence of a downfield shift with



added pyridine confirms that these aggregates are unsolvated. They are also demonstrably lower aggregates than hexamers (*vide supra*) and larger than observable dimers (*vide infra*). A plot of  $n$ -mer versus hexamer at various enolate concentrations afforded a value of  $n$  consistent with a tetramer (Figure 10). Efforts to use MCV failed, however, owing to poor resolution.

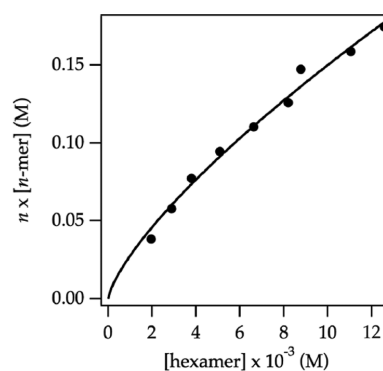


**Figure 10.** A plot of  $n \times n$ -mer concentration versus hexamer concentration for **1a** in toluene at  $-70$  °C. The plot was fitted to  $y = n(K_{eq}^{1/6}x^{n/6})$ , affording  $n = 4.4 \pm 0.2$  and confirming the lower aggregate as a tetramer. The derivation is found in the Supporting Information.

DFT computations at the B3LYP/6-31G(d) level of theory with single-point calculations at the MP2 level of theory<sup>20,21</sup> were brought to bear on the problem. The numbers are reported in kilocalories per mole per lithium.<sup>20,21</sup> The hexamers are considerably more stable than the tetramers (eq 3), which conflicts with the nearly thermoneutral relationship observed experimentally.  $S_6$ -symmetric hexamer **8a** and  $D_{3d}$  tetramer **9a** are equivalent within computational error (eq 4).<sup>22</sup>  $S_4$ -symmetric tetramer **7a** is slightly less stable than the  $D_{2d}$  form, **15a** (eq 5). Compared with both the hexamer and tetramer, the unsolvated dimer (not shown) is much higher in energy, which suggests that the unsolvated dimer is an improbable form.

**Solution Structures: THF.** In 1.0–4.0 M THF/toluene, the incremental addition of THF to enolate **1a** converts the hexamer–tetramer mixture to a single new aggregate (Figure 11) shown to be a solvated dimer by MCV (below). Incremental addition of pyridine to **1a** in 1.0 M THF/toluene causes a marked downfield shift that confirms the solvated form of the dimer. The spectrum of [<sup>6</sup>Li,<sup>15</sup>N]**1a** fails to show clear <sup>6</sup>Li–<sup>15</sup>N coupling at temperatures as low as  $-115$  °C, which is consistent with a loss of chelation, but some broadening of the <sup>6</sup>Li resonance suggests that a dynamic process is involved. Indeed, the <sup>6</sup>Li resonance of the *ethoxy*-substituted enolate [<sup>6</sup>Li,<sup>15</sup>N]**1b** appears as a triplet owing to <sup>6</sup>Li–<sup>15</sup>N coupling ( $J = 1.5$  Hz). The lone triplet suggests rapid intra-aggregate chelate exchange with the concomitant appearance of coupling by both <sup>6</sup>Li–<sup>15</sup>N dative interactions (eq 6) statistically averaged to half the normal 3 Hz coupling.<sup>16</sup>

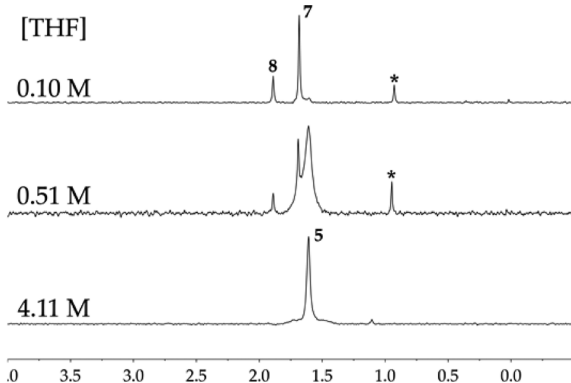
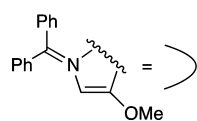
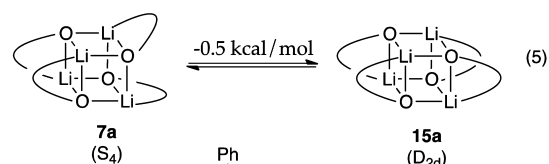
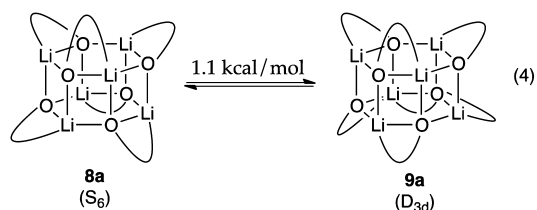
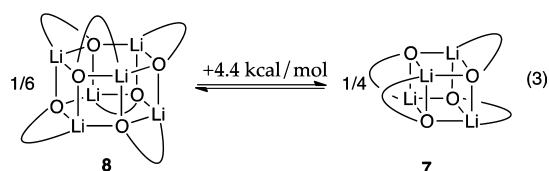
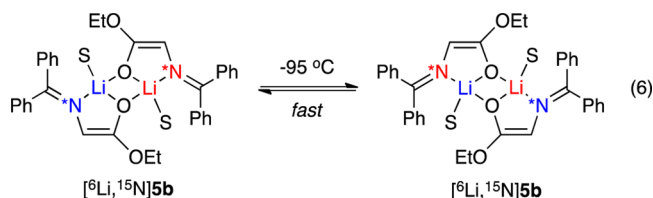


**Figure 11.**  $^6\text{Li}$  NMR spectra of 0.10 M  $[\text{}^6\text{Li}]$  **1a** in various THF/toluene concentrations showing the symmetric dimer **5a**, tetramer **7a**, and hexamer **8a**. From top to bottom, the spectra were obtained at  $-70$ ,  $-70$ , and  $-90$   $^\circ\text{C}$ , respectively. The asterisks denote lithium hexamethyldisilazide.



The spectrum of alanine-derived enolate **2a** in THF/toluene solution is different than that of **1a** (*vide infra*). Most important, distinctly different chemical shifts for **1a** and **2a** allow for an MCV analysis. Thus, varying the mole fraction of enolates **1a** and **2a** affords an ensemble of resonances consistent with dimeric homoaggregates and a single heteroaggregate (Figure 12). The resulting Job plot is illustrated in Figure 13. Heterodimer **16** should appear as two distinct  $^6\text{Li}$  resonances, but the rapid chelate exchange akin to that in eq 6 precludes this result.

A critical consequence of the time-averaging is our inability to distinguish symmetric dimer **5a** from unsymmetric dimer **6a**.

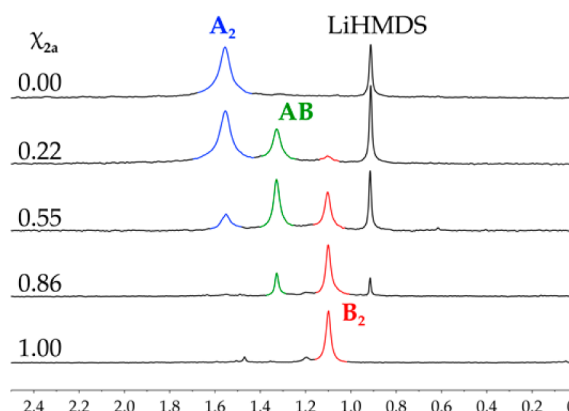


**Figure 12.**  $^6\text{Li}$  NMR spectra showing the dimer ensemble of **1a** ( $A_2$ ) and **2a** ( $B_2$ ). The total enolate concentration is 0.10 M in 1.00 M THF at  $-75$   $^\circ\text{C}$ .  $\chi_{2a}$  indicates the measured mole fractions of **2a**.

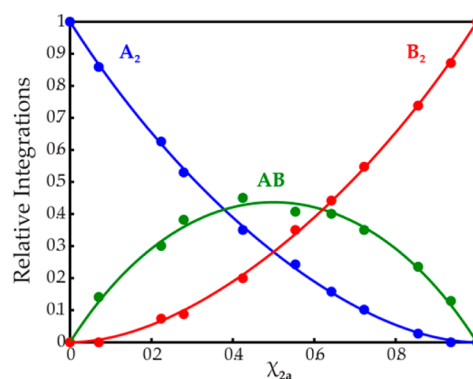
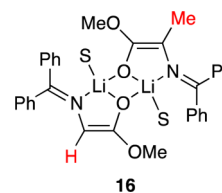
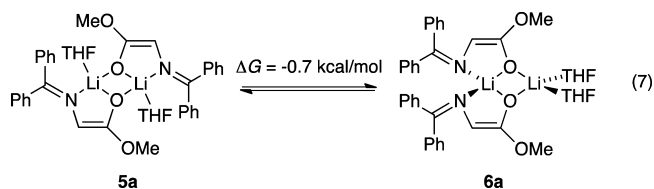


**Figure 13.** Job plot showing the relative integrations of dimeric homo- and heteroaggregates versus  $\chi_{2a}$  for 0.10 M mixtures of **1a** ( $A_2$ ) and **2a** ( $B_2$ ) at  $-75$   $^\circ\text{C}$ .



DFT computations weigh in by showing that they are of nearly equal stability (eq 7). The role of type **6** dimers comes to light with chelating ligands (*vide infra*).



Solutions of **1a** in 8.0 M THF show dimers along with a minor upfield shoulder below  $-80$   $^\circ\text{C}$  that is suspected to be a monomer. The more substituted alanine-derived enolate **2a** shows the putative monomer resonance slightly downfield, but it is better resolved and the dominant form in neat THF. Reducing the enolate concentration and lowering the temperature also favored monomer relative to dimer.<sup>23</sup> Monitoring the dimer–monomer equilibrium versus absolute concentration affords further support of the monomer assignment (Figure 14).

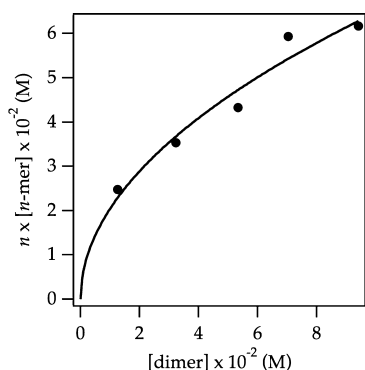
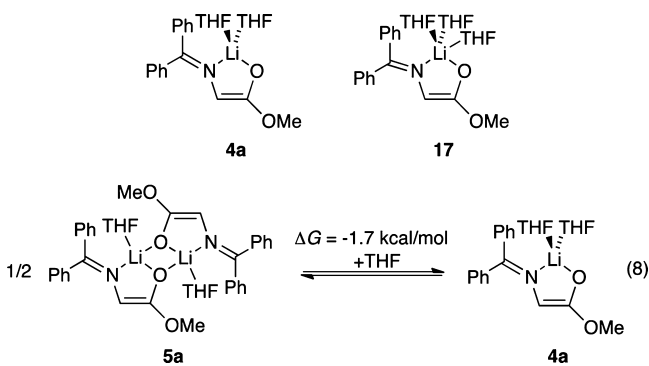


**Figure 14.** Plot of  $n \times [n\text{-mer}]$  vs  $[\text{dimer}]$  for **2a** in 6.0 M THF at  $-90\text{ }^\circ\text{C}$ . The best fit gives  $n = 1.0 \pm 0.2$ , confirming the lower aggregate as a monomer. The plot was fitted to  $y = n(K_{\text{eq}}^{1/2} x^{n/2})$ , derived in the [Supporting Information](#).

Unfortunately, exchange occurs too quickly to observe  ${}^6\text{Li}\text{--}{}^{15}\text{N}$  coupling at  $-90\text{ }^\circ\text{C}$ .

Conventional thinking that presumes tetrahedral lithium suggests the monomer to be disolvate **4a**, but five-coordinate monomer **17** seems reasonable to us in light of well-documented high-coordinate lithium.<sup>24</sup> Nonetheless, **17** is not computationally viable (expels a THF ligand), possibly owing to crowding by the phenyl moiety. The computations show a modest preference for the dimeric form (eq 8).



Camphor-derived enolates **3** exhibit markedly different behaviors. The unsolvated hexamer **9a** derived from enolate **3a** is observable even in neat THF solution and at elevated temperatures, affording only low concentrations of a THF-solvated form of unknown structure. The  ${}^6\text{Li}$  NMR spectrum of ethyl ester-derived enolate **3b** in THF is intractable; the *tert*-butyl ester-derived enolate **3c** is more tractable but still complex. The steric inhibition of solvation is likely at play.<sup>25</sup>

**Solution Structures: TMEDA.** Despite having a crystal structure of **5b** bearing an  $\eta^1$ -TMEDA (Figure 2), we could not detect symmetric type **5** dimers in significant concentrations. By contrast, unsymmetrical dimer **6a**, which lacks crystallographic analogy within our study, is quite prevalent. The spectroscopic properties arising from the symmetry of **6** are definitive (Figure 15).<sup>26</sup>

Results for enolates **1a** and **1b** are analogous; maximal resolution is observed with ethyl ester derived enolate **1b** (Figure 16). Dimer **6b** displays two distinct  ${}^6\text{Li}$  resonances. The downfield resonance at 2.94 ppm splits into a triplet ( $J_{\text{Li--N}} = 3.0\text{ Hz}$ ) for  ${}^{[6}\text{Li}, {}^{15}\text{N}]$ **1b**, whereas the upfield peak at 0.72 ppm is a singlet. The  ${}^6\text{Li}$  resonances maintain 1:1 ratios under all conditions. High concentrations of TMEDA cause the disappearance of **6b** and the growth of putative monomer **4b**.

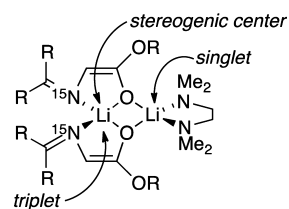


**Figure 15.** Generic structure of a type **6** dimer illustrating characteristic splitting patterns and stereochemistry.

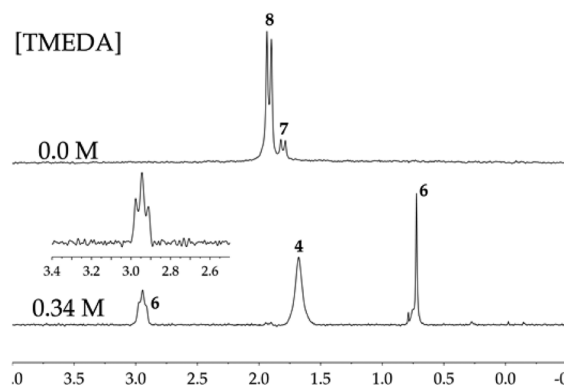
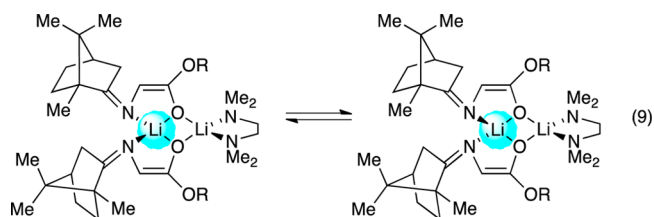


**Figure 16.**  ${}^6\text{Li}$  NMR spectra of  ${}^{[6}\text{Li}, {}^{15}\text{N}]$ **1b** in neat toluene (top) and in 0.34 M TMEDA/toluene (bottom) at  $-75\text{ }^\circ\text{C}$ . Inset:  ${}^6\text{Li}$  resonance of **6** with additional window functions showing the splitting by two  ${}^{15}\text{N}$  nuclei.

As depicted in Figure 15, the spirocyclic structure of **6** renders the internal lithium nucleus stereogenic with concomitant formation of *diastereomers* of camphor-derived enolates **3a–c** (eq 9).  ${}^{[6}\text{Li}]$ **3b** at low TMEDA concentrations in toluene gave



the clearest resolution of dimer **6** as an approximate 3:1 mixture of diastereomers (Figure 17a). The two upfield resonances, each corresponding to a diastereomer, resolve for enolates **3a–c**, whereas the downfield resonances corresponding to the stereogenic centers offer only glimpses of doubling in the form of distortions. The 1:1 ratio was shown to be constant by integrating the pairs of upfield resonances and the broad downfield resonance. The downfield resonances of enolates  ${}^{[6}\text{Li}, {}^{15}\text{N}]$ **3a** and  ${}^{[6}\text{Li}, {}^{15}\text{N}]$ **3b** appear as broadened (superimposed) triplets, whereas neither splitting nor broadening was observed for the two upfield resonances.

Solutions of enolate  ${}^{[6}\text{Li}, {}^{15}\text{N}]$ **3b** observed at high TMEDA concentration afford a new species consistent with monomer **4b**. In contrast to the benzophenone-based enolates in which coupling is not observable, camphor-derived monomer **4b** appears as a doublet ( $J_{\text{Li--N}} = 4.2\text{ Hz}$ ). Thus, the assignment as a monomer is reasonably secure, although we cannot rigorously exclude a higher symmetric oligomer such as dimer **5**.

**Solution Structures: *N,N,N',N'*-Tetramethylcyclohexanediamine (TMEDA).** In analogy with TMEDA, TMEDA<sup>27,28</sup> influences the aggregation of enolates **1–3**. The

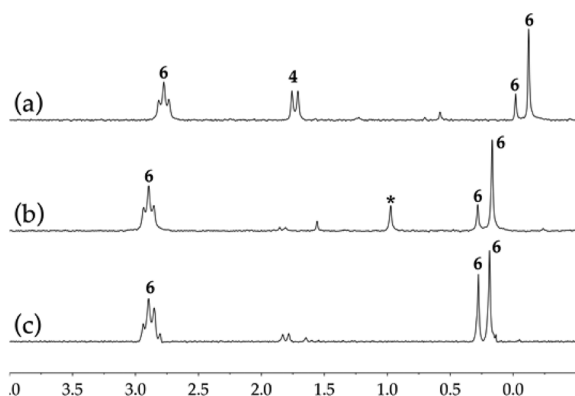
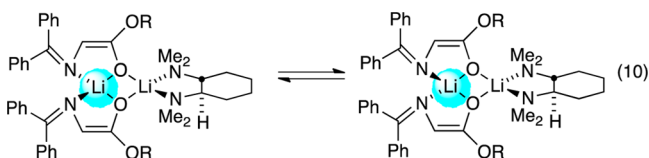


**Figure 17.**  ${}^6\text{Li}$  NMR spectra of  $[{}^6\text{Li}, {}^{15}\text{N}]\mathbf{3b}$  at  $-95\text{ }^\circ\text{C}$  in (a) 0.55 M TMEDA; (b) 0.48 M (*R,R*)-*N,N,N',N'*-tetramethylcyclohexanediamine [(*R,R*)-TMEDA]; and (c) 0.48 M (*S,S*)-TMEDA in toluene cosolvent. The downfield resonances of the type **6** dimer in (*S,S*)-TMEDA clearly display the overlapping triplets, whereas TMEDA and (*R,R*)-TMEDA show only the resolution of the upfield resonances.

chirality is clarifying but offers one confounding result. Benzophenone derivative **1a** in (*R,R*)-TMEDA/toluene shows a number of  ${}^6\text{Li}$  resonances consistent with dimers **6** in which the stereogenic center at lithium causes the formation of diastereomers (eq 10). The upfield resonances resolve, whereas the



downfield resonances do not. There was added complexity, however. The integrations of the upfield resonances do not match those of downfield peaks, and this outcome suggests an aggregate of unknown structure hiding underneath. The ethyl ester enolate **1b** provides improved resolution, although the amount of dimer **6b** is not as significant owing to the appearance of monomer at relatively low TMEDA concentrations.

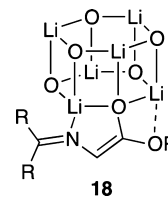
The confounding result is that we observe *three* pairs of  ${}^6\text{Li}$  resonances of **6b** with matching integration values in the presence of 0.040 M (*S,S*)-TMEDA. The downfield  ${}^6\text{Li}$  resonances of  $[{}^6\text{Li}, {}^{15}\text{N}]\mathbf{1b}$  appear as overlapping multiplets, and the upfield resonances are partially resolved. The putative monomer appears at 1.80 ppm with  ${}^6\text{Li}$ – ${}^{15}\text{N}$  coupling (2.9 Hz) as expected. The remaining benzophenone derivatives **1c** and **2a** show strong tendencies to form monomers.

The camphor derivatives **3** do not afford a detectable monomer. Solvation of enolate **3a** by (*R,R*)-TMEDA affords unsymmetric type **6** dimers more readily than that by TMEDA. The unsolvated hexamer persists in various degrees throughout a series of TMEDA concentrations ranging from 0.048 to 1.80 M. Labeling studies of **3a** show what appears to be superimposed triplets along with unaffected singlets in the upfield region. (*S,S*)-TMEDA affords an unsymmetric dimer with distinctly different chemical shifts (as expected). The resolution is maximized by using the ethoxy derivative (Figure 17b,c) wherein  $[{}^6\text{Li}, {}^{15}\text{N}]\mathbf{3b}$  shows two pairs of  ${}^6\text{Li}$  resonances manifesting two triplet–singlet pairs in the presence of (*S,S*)-TMEDA.

## DISCUSSION

Lithium enolates **1–3** derived from glycinimines are synthetically useful for preparing non-natural substituted amino acids.<sup>1–4</sup> A clear understanding of organolithium solvation and aggregation is a *mandatory* prerequisite for elucidating the mechanistic basis of stereocontrol: the solvent-dependent structure determinations described herein represent the first steps toward understanding how structure influences mechanism and reactivity. The crystallographic studies revealed an unusually diverse array of aggregate types (Chart 1). Spectroscopic studies showed a high but imperfect correlation between solid-state and solution structures. Computational studies provided a few experimentally elusive details and theory–experiment correlations.

**Hexamers.** Ligand-free hexamers characterized crystallographically and shown by MCV to persist in toluene solutions have several curious structural features. The most surprising is that the benzophenone-derived enolate (see Figure 5) and camphor-derived enolate (see Figure 6) prefer fundamentally different  $S_6$ - and  $D_{3d}$ -symmetric core structures (**8** and **9**), respectively. The stereochemistry of the hexamers in solution is elusive, but tacit evidence suggests the chiral camphor-derived hexamer is  $D_{3d}$ -symmetric **9**. The ethoxy–lithium interactions (**18**) could be attributable to steric relief but are also likely to be stabilizing. We suspect that the approximate  $120^\circ$  Li–O–Li bond angle of the hexagonal prism may support the multidentate contact, whereas the more acute angles on lower aggregates do not.



**Tetramers.** The tetramers were the most elusive of the structural forms. A crystallographically characterized  $S_4$  isomer (Figure 4) was observed, but computations of enolate **1a** indicate a preference for the  $D_{2d}$  isomer **15** (eq 5). Both forms of chelating organolithiums are precedented.<sup>29,30</sup> Computations also showed a distinct preference for hexamers over tetramers. Tetramers were detected in solution, but the assignment were inferred from concentration dependencies. All attempts to apply MCV analysis failed to identify pairing partners that would afford well-resolved ensembles.

**Dimers.** The dimeric enolates underscored the divergence of solution and solid-state structures: symmetric dimers of type **5** were observed (twice) crystallographically (Figures 2 and 3) but in many instances could not be unassailably identified in solution. By contrast, unsymmetric type **6** dimers were readily detected and characterized in solution owing to their highly characteristic resonance counts and  ${}^6\text{Li}$ – ${}^{15}\text{N}$  coupling patterns, but none crystallized. Both **5** and **6** are computationally viable (eq 7) and have ample analogy in the structural organolithium literature.<sup>23</sup>

The stereogenic center of the **6** type dimer (see Figure 15) offered interesting spectroscopic properties in that introducing additional stereogenic centers by using camphor-derived enolates **3**, (*R,R*)-TMEDA, or (*S,S*)-TMEDA resulted in peak doublings consistent with mixtures of diastereomers (eqs 9 and 10).

**Monomers.** A monomer of enolate **4c** chelated by TMEDA was characterized crystallographically (Figure 1). Toluene

solutions containing THF, TMEDA, and TMCDA all afforded putative monomers at high ligand concentrations. Rapid exchanges, however, caused a loss of the expected  ${}^6\text{Li}$ – ${}^{15}\text{N}$  coupling in most circumstances, although we did see coupling in one case. We are comfortable assigning TMEDA- and TMCDA-solvated monomers as four-coordinated chelates in solution. We suspected that the THF solvates might favor five-coordinate forms **17** owing to well-precedented high-coordinate lithium. Computational studies clearly do not support this notion, however.

## CONCLUSION

Glycinimine-derived enolates provide unexpectedly rich structural diversity when solvated by several standard solvents. The various aggregates necessarily influence the rates of alkylation. It is less clear, however, whether the different species influence the stereochemistries of functionalizations. Aggregate-dependent mechanisms and stereochemistries depend on whether the aggregates react with electrophiles without intervening deaggregations or whether they all funnel through common, possibly monomer-based, intermediates. We have some evidence that the aggregates can react directly, but these studies are preliminary, ongoing, and challenging.

## EXPERIMENTAL SECTION

**Reagents and Solvents.** Glycinimines were prepared from the corresponding commercially available glycinate esters,  ${}^{15}\text{N}$ -labeled glycinate esters, benzophenone, camphor, and thiocamphor via literature protocols.<sup>3a,h</sup> Toluene, hexanes, TMEDA, THF, (*R,R*)-*trans*-TMCDA,<sup>27</sup> and (*S,S*)-*trans*-TMCDA<sup>27</sup> were distilled from sodium benzophenone ketyl. Toluene and hexanes were distilled from blue solutions containing sodium benzophenone ketyl with approximately 1% tetraglyme to dissolve the ketyl. [ ${}^6\text{Li}$ ]LiHMDS and [ ${}^6\text{Li}$ , ${}^{15}\text{N}$ ]-LiHMDS were prepared and recrystallized as described previously.<sup>7</sup> Air- and moisture-sensitive materials were manipulated under argon using standard glovebox, vacuum line, and syringe techniques.

**NMR Spectroscopy.** Individual stock solutions of substrates and base were prepared at room temperature. An NMR tube under vacuum was flame-dried on a Schlenk line and allowed to return to room temperature. It was then backfilled with argon and placed in a  $-78\text{ }^\circ\text{C}$  dry ice/acetone bath. The appropriate amounts of [ ${}^6\text{Li}$ ]LiHMDS and glycinimine were added sequentially via syringe. The tube was sealed under partial vacuum, aged at  $25\text{ }^\circ\text{C}$  for  $\geq 60$  min to equilibrate the aggregates, stored in a  $-86\text{ }^\circ\text{C}$  freezer until used to record the spectra, and shaken before placement into the spectrometer. Each NMR sample contained 0.10 M total enolate and 0.11 M LiHMDS unless stated otherwise.

${}^6\text{Li}$  NMR spectra were typically recorded at temperatures between  $-70$  and  $-80\text{ }^\circ\text{C}$  on a 500 or 600 MHz spectrometer with the delay between scans set to  $>5 \times T_1$  to ensure accurate integrations. Chemical shifts were reported relative to a 0.30 M  ${}^6\text{LiCl}/\text{MeOH}$  standard at the reported probe temperature. The resonances were integrated by using the standard software accompanying the spectrometers. After weighted Fourier transform with 64 000 points and phasing, line broadening was set between 0 and 0.3, and a baseline correction was applied when appropriate. Deconvolution of the ensemble in the experiments for MCV determination of structure was performed in the absolute intensity mode, with the application of a drift correction using default parameters for contributions from Lorentzian and Gaussian line shapes. The mathematics underlying the parametric fits have been described in detail.<sup>15a</sup>

## ASSOCIATED CONTENT

### Supporting Information

The Supporting Information is available free of charge on the ACS Publications website at DOI: 10.1021/jacs.5b09524.

Crystallographic data for **4c** (CIF)

Crystallographic data for TMEDA-solvated **5b** (CIF)

Crystallographic data for THF-solvated **5b** (CIF)

Crystallographic data for **7a** (CIF)

Crystallographic data for **8b** (CIF)

Crystallographic data for **9a** (CIF)

Crystallographic, spectroscopic, and computational data and authors for ref **20** (PDF)

## AUTHOR INFORMATION

### Corresponding Author

\*dbc6@cornell.edu

### Notes

The authors declare no competing financial interest.

## ACKNOWLEDGMENTS

We thank the National Institutes of Health (GM077167).

## REFERENCES

- (1) (a) Abellán, T.; Chinchilla, R.; Galindo, N.; Guillena, G.; Nájera, C.; Sansano, J. M. *Eur. J. Org. Chem.* **2000**, 15, 2689.
- (2) (a) O'Donnell, M. J. *Acc. Chem. Res.* **2004**, 37, 506. (b) O'Donnell, M. J.; Wu, S.; Huffman, J. C. *Tetrahedron* **1994**, 50, 4507. (c) O'Donnell, M. J.; Wu, S. *Tetrahedron: Asymmetry* **1992**, 3, 591. (d) Lygo, B.; Andrews, B. *Acc. Chem. Res.* **2004**, 37, 518. (e) Ooi, T.; Maruoka, K. *Angew. Chem., Int. Ed.* **2007**, 46, 4222. (f) Maruoka, K. *Org. Process Res. Dev.* **2008**, 12, 679. (g) Maruoka, K.; Ooi, T. *Chem. Rev.* **2003**, 103, 3013.
- (3) (a) McIntosh, J. M.; Mishra, P. *Can. J. Chem.* **1986**, 64, 726. (b) McIntosh, J. M.; Leavitt, R. K. *Tetrahedron Lett.* **1986**, 27, 3839. (c) McIntosh, J. M.; Cassidy, K. C. *Can. J. Chem.* **1988**, 66, 3116. (d) McIntosh, J. M.; Leavitt, R. K.; Mishra, P.; Cassidy, K. C.; Drake, J. E.; Chadha, R. J. *Org. Chem.* **1988**, 53, 1947. (e) Sánchez-Obregón, R.; Fallis, A. G.; Szabo, A. G. *Can. J. Chem.* **1992**, 70, 1531. (f) Laue, K. W.; Mück-Lichtenfeld, C.; Haufe, G. *Tetrahedron* **1999**, 55, 10413. (g) Kroeger, S.; Haufe, G. *Liebigs Annalen/Recueil.* **1997**, 1997, 1201. (h) O'Donnell, M. J.; Polt, R. L. *J. Org. Chem.* **1982**, 47, 2663–2666.
- (4) (a) Kanemasa, S.; Tatsukawa, A.; Wada, E. *J. Org. Chem.* **1991**, 56, 2875. (b) Yamamoto, H.; Kanemasa, S.; Wada, E. *Bull. Chem. Soc. Jpn.* **1991**, 64, 2739. (c) Tatsukawa, A.; Dan, M.; Ohbatake, M.; Kawatake, K.; Fukata, T.; Wada, E.; Kanemasa, S.; Kakei, S. *J. Org. Chem.* **1993**, 58, 4221. (d) Pyne, S. G.; Safaei-G, J.; Schafer, K.; Javidan, A.; Skelton, B. W.; White, A. H. *Aust. J. Chem.* **1998**, 51, 137. (e) Changyou, Z.; Daimo, C.; Yaozhong, J. *Synth. Commun.* **1987**, 17, 1377. (f) Tatsukawa, A.; Kawatake, K.; Kanemasa, S.; Rudzinski, J. M. *J. Chem. Soc., Perkin Trans. 2* **1994**, 2525. (g) Kanemasa, S.; Tatsukawa, A.; Wada, E.; Tsuge, O. *Chem. Lett.* **1989**, 18, 1301.
- (5) (a) Green, J. R. *Science of Synthesis*; Georg Thieme Verlag: New York, 2005; Vol. 8a, pp 427–486. (b) Schetter, B.; Mahrwald, R. *Angew. Chem., Int. Ed.* **2006**, 45, 7506. (c) Arya, P.; Qin, H. *Tetrahedron* **2000**, 56, 917. (d) Caine, D. In *Comprehensive Organic Synthesis*; Trost, B. M., Fleming, I., Eds.; Pergamon: New York, 1989; Vol. 1, p 1. (e) Martin, S. F. *Ibid.*, Vol. 1, p 475. (f) Plaquevent, J.-C.; Cahard, D.; Guillen, F.; Green, J. R. *Science of Synthesis*; Georg Thieme Verlag: New York, 2005; Vol. 26, pp 463–511. (g) *Comprehensive Organic Functional Group Transformations II*; Katritzky, A. R., Taylor, R. J. K., Eds.; Elsevier: Oxford, U.K., 1995; pp 834–835. (h) Cativiela, C.; Diaz-de-Villegas, M. D. *Tetrahedron: Asymmetry* **2007**, 18, 569. (i) Dugger, R. W.; Ragan, J. A.; Ripin, D. H. B. *Org. Process Res. Dev.* **2005**, 9, 253. (j) Farina, V.; Reeves, J. T.; Senanayake, C. H.; Song, J. J. *Chem. Rev.* **2006**, 106, 2734. (k) Wu, G.; Huang, M. *Chem. Rev.* **2006**, 106, 2596.
- (6) (a) Seebach, D. *Angew. Chem., Int. Ed. Engl.* **1988**, 27, 1624. (b) Reich, H. J. *Chem. Rev.* **2013**, 113, 7130. (c) Braun, M. *Helv. Chim. Acta* **2015**, 98, 1. (d) Setzer, W. N.; Schleyer, P. v. R. *Adv. Organomet. Chem.* **1985**, 24, 353. (e) Williard, P. G. In *Comprehensive Organic Synthesis*; Trost, B. M., Fleming, I., Eds.; Pergamon: New York, 1991; Vol. 1, Chapter 1.1. (f) Reich, H. J. *J. Org. Chem.* **2012**, 77, 5471.



- (g) Kim, Y.-J.; Streitwieser, A. *Org. Lett.* **2002**, *4*, 573. (h) Jackman, L. M.; Lange, B. C. *Tetrahedron* **1977**, *33*, 2737. (i) Li, D.; Keresztes, I.; Hopson, R.; Williard, P. G. *Acc. Chem. Res.* **2009**, *42*, 270. (j) Zune, C.; Jerome, R. *Prog. Polym. Sci.* **1999**, *24*, 631. (k) Baskaran, D. *Prog. Polym. Sci.* **2003**, *28*, 521.
- (7) Romesberg, F. E.; Bernstein, M. P.; Gilchrist, J. H.; Harrison, A. T.; Fuller, D. J.; Collum, D. B. *J. Am. Chem. Soc.* **1993**, *115*, 3475.
- (8) (a) Bauer, W.; Klusener, P. A. A.; Harder, S.; Kanters, J. A.; Duisenberg, A. J. M.; Brandsma, L.; Schleyer, P. v. R. *Organometallics* **1988**, *7*, 552. (b) Köster, H.; Thoenes, D.; Weiss, E. *J. Organomet. Chem.* **1978**, *160*, 1. (c) Tecle, B.; Ilsley, W. H.; Oliver, J. P. *Organometallics* **1982**, *1*, 875. (d) Harder, S.; Boersma, J.; Brandsma, L.; Kanters, J. A. *J. Organomet. Chem.* **1988**, *339*, 7. (e) Sekiguchi, A.; Tanaka, M. *J. Am. Chem. Soc.* **2003**, *125*, 12684. (f) Linnert, M.; Bruhn, C.; Ruffer, T.; Schmidt, H.; Steinborn, D. *Organometallics* **2004**, *23*, 3668. (g) Fraenkel, G.; Stier, M. *Prepr. Am. Chem. Soc., Div. Pet. Chem.* **1985**, *30*, 586. (h) Ball, S. C.; Cragg-Hine, I.; Davidson, M. G.; Davies, R. P.; Lopez-Solera, M. I.; Raithby, P. R.; Reed, D.; Snaith, R.; Vogl, E. M. *J. Chem. Soc., Chem. Commun.* **1995**, 2147. (i) Wehman, E.; Jastrzebski, J. T. B. H.; Ernsting, J.-M.; Grove, J. M.; van Koten, G. *J. Organomet. Chem.* **1988**, *353*, 145. (j) Becker, J.; Grimme, S.; Fröhlich, R.; Hoppe, D. *Angew. Chem., Int. Ed.* **2007**, *46*, 1645. (k) Bernstein, M. P.; Romesberg, F. E.; Fuller, D. J.; Harrison, A. T.; Williard, P. G.; Liu, Q. Y.; Collum, D. B. *J. Am. Chem. Soc.* **1992**, *114*, 5100.
- (9) Collum, D. B. *Acc. Chem. Res.* **1992**, *25*, 448.
- (10) (a) Hexamethyldisiloxane is reputed to be less polar than standard hydrocarbons for crystallizing lipophilic compounds (ref 10b). For organolithium reagents, the more robust tetramethylsilane appears to act similarly as evidenced by the insolubility of LiHMDS (ref 10c). (b) Pfeifer, J. Hexamethyldisiloxane. In *Encyclopedia of Reagents for Organic Synthesis*; Paquette, L. A., Ed.; Wiley: New York, 2004. (c) Lucht, B. L.; Collum, D. B. *J. Am. Chem. Soc.* **1996**, *118*, 2217.
- (11) (a) Collum, D. B. *Acc. Chem. Res.* **1993**, *26*, 227. (b) Lucht, B. L.; Collum, D. B. *Acc. Chem. Res.* **1999**, *32*, 1035.
- (12) Mulvey, R. E. *Chem. Soc. Rev.* **1991**, *20*, 167.
- (13) Bruneau, A. M.; Collum, D. B. *J. Am. Chem. Soc.* **2014**, *136*, 2885.
- (14) Renny, J. S.; Tomasevich, L. L.; Tallmadge, E. H.; Collum, D. B. *Angew. Chem., Int. Ed.* **2013**, *52*, 11998.
- (15) (a) Liou, L. R.; McNeil, A. J.; Ramirez, A.; Toombes, G. E. S.; Gruver, J. M.; Collum, D. B. *J. Am. Chem. Soc.* **2008**, *130*, 4859. (b) De Vries, T. S.; Goswami, A.; Liou, L. R.; Gruver, J. M.; Jayne, E.; Collum, D. B. *J. Am. Chem. Soc.* **2009**, *131*, 13142. (c) Liou, L. R.; McNeil, A. J.; Toombes, G. E. S.; Collum, D. B. *J. Am. Chem. Soc.* **2008**, *130*, 17334.
- (16) (a) Arvidsson, P. I.; Ahlberg, P.; Hilmersson, G. *Chem. - Eur. J.* **1999**, *5*, 1348. (b) Bauer, W. *J. Am. Chem. Soc.* **1996**, *118*, 5450. (c) Bauer, W.; Griesinger, C. *J. Am. Chem. Soc.* **1993**, *115*, 10871. (d) DeLong, G. T.; Pannell, D. K.; Clarke, M. T.; Thomas, R. D. *J. Am. Chem. Soc.* **1993**, *115*, 7013. (e) Thomas, R. D.; Clarke, M. T.; Jensen, R. M.; Young, T. C. *Organometallics* **1986**, *5*, 1851. (f) Bates, T. F.; Clarke, M. T.; Thomas, R. D. *J. Am. Chem. Soc.* **1988**, *110*, 5109. (g) Fraenkel, G.; Hsu, H.; Su, B. M. In *Lithium: Current Applications in Science, Medicine, and Technology*; Bach, R. O., Ed.; Wiley: New York, 1985; pp 273–289. (h) Heinzer, J.; Oth, J. F. M.; Seebach, D. *Helv. Chim. Acta* **1985**, *68*, 1848. (i) Fraenkel, G.; Henrichs, M.; Hewitt, J. M.; Su, B. M.; Geckle, M. J. *J. Am. Chem. Soc.* **1980**, *102*, 3345. (j) Lucht, B. L.; Collum, D. B. *J. Am. Chem. Soc.* **1996**, *118*, 3529. (k) Knorr, R.; Menke, T.; Ferchland, K.; Mehlstäubel, J.; Stephenson, D. S. *J. Am. Chem. Soc.* **2008**, *130*, 14179.
- (17) Job, P. *Ann. Chim.* **1928**, *9*, 113.
- (18) (a) Tomasevich, L. L.; Collum, D. B. *J. Org. Chem.* **2013**, *78*, 7498. (b) Reich, H. J.; Kulicke, K. J. *J. Am. Chem. Soc.* **1996**, *118*, 273. (c) Jackman, L. M.; Chen, X. *J. Am. Chem. Soc.* **1997**, *119*, 8681. (d) Jackman, L. M.; Petrei, M. M.; Smith, B. D. *J. Am. Chem. Soc.* **1991**, *113*, 3451. (e) Jackman, L. M.; DeBrosse, C. W. *J. Am. Chem. Soc.* **1983**, *105*, 4177. (f) Dean, R. K.; Reckling, A. M.; Chen, H.; Dawe, L. N.; Schneider, C. M.; Kozak, C. M. *Dalton Trans.* **2013**, *42*, 3504. (g) Boyle, T. J.; Pedrotty, D. M.; Alam, T. M.; Vick, S. C.; Rodriguez, M. A. *Inorg. Chem.* **2000**, *39*, 5133.
- (19) The measured mole fraction—the mole fraction within only the ensemble of interest—rather intended mole fraction of the enolates added to the samples—eliminates the distorting effects of impurities.
- (20) Frisch, M. J.; et al. *Gaussian*, version 3.09; revision A.1; Gaussian, Inc.: Wallingford, CT, 2009.
- (21) For leading references to theoretical studies of O-lithiated species, see: (a) Khartabil, H. K.; Gros, P. C.; Fort, Y.; Ruiz-Lopez, M. F. *J. Org. Chem.* **2008**, *73*, 9393. (b) Streitwieser, A. *J. Mol. Model.* **2006**, *12*, 673. (c) Pratt, L. M.; Streitwieser, A. *J. Org. Chem.* **2003**, *68*, 2830. (d) Pratt, L. M.; Nguyen, S. C.; Thanh, B. T. *J. Org. Chem.* **2008**, *73*, 6086.
- (22) Because of technical problems owing to their size, the hexamer comparison in eq 4 is not MP2 corrected.
- (23) Reich, H. J. *Chem. Rev.* **2013**, *113*, 7130.
- (24) (a) Lucht, B. L.; Collum, D. B. *J. Am. Chem. Soc.* **1995**, *117*, 9863. (b) Scheschke, D. *Angew. Chem., Int. Ed.* **2004**, *43*, 2965. (c) Niecke, E.; Nieger, M.; Schmidt, O.; Gudat, D.; Schoeller, W. W. *J. Am. Chem. Soc.* **1999**, *121*, 519. (d) Becker, G.; Eschbach, B.; Mundt, O.; Reti, M.; Niecke, E.; Issberner, K.; Nieger, M.; Thelen, V.; Noth, H.; Waldhor, R.; Schmidt, M. Z. *Anorg. Allg. Chem.* **1998**, *624*, 469. (e) Becker, G.; Schwarz, W.; Seidler, N.; Westerhausen, M. Z. *Anorg. Allg. Chem.* **1992**, *612*, 72. (f) Wang, H.; Wang, H.; Li, H.-W.; Xie, Z. *Organometallics* **2004**, *23*, 875. (g) Xu, X.; Zhang, Z.; Yao, Y.; Zhang, Y.; Shen, Q. *Inorg. Chem.* **2007**, *46*, 9379. (h) Thiele, K.; Gorls, H.; Imhof, W.; Seidel, W. Z. *Anorg. Allg. Chem.* **2002**, *628*, 107. (i) Ramirez, A.; Lobkovsky, E.; Collum, D. B. *J. Am. Chem. Soc.* **2003**, *125*, 15376. (j) Buchalski, P.; Grabowska, I.; Kaminska, E.; Suwinska, K. *Organometallics* **2008**, *27*, 2346.
- (25) (a) Zhao, P.; Collum, D. B. *J. Am. Chem. Soc.* **2003**, *125*, 14411 and references cited therein. (b) For an early suggestion that steric effects are major determinants of solvation, see: Settle, F. A.; Haggerty, M.; Eastham, J. F. *J. Am. Chem. Soc.* **1964**, *86*, 2076. (c) Bernstein, M. P.; Collum, D. B. *J. Am. Chem. Soc.* **1993**, *115*, 8008.
- (26) (a) Reich, H. J.; Goldenberg, W. S.; Gudmundsson, B. Ö.; Sanders, A. W.; Kulicke, K. J.; Simon, K.; Guzei, I. A. *J. Am. Chem. Soc.* **2001**, *123*, 8067. (b) Steiner, A.; Stalke, D. *Angew. Chem., Int. Ed. Engl.* **1995**, *34*, 1752. (c) Belzner, J.; Schar, D.; Dehnert, U.; Noltemeyer, M. *Organometallics* **1997**, *16*, 285. (d) Jantzi, K. L.; Puckett, C. L.; Guzei, I. A.; Reich, H. J. *J. Org. Chem.* **2005**, *70*, 7520. (e) Vos, M.; de Kanter, F. J. J.; Schakel, M.; van Eikema Hommes, N. J. R.; Klumpp, G. W. *J. Am. Chem. Soc.* **1987**, *109*, 2187. (f) Hilmersson, G.; Davidsson, O. *J. Org. Chem.* **1995**, *60*, 7660. (g) Hilmersson, G.; Arvidsson, P. I.; Davidsson, Ö.; Håkansson, M. *Organometallics* **1997**, *16*, 3352. (h) Hilmersson, G. *Chem. - Eur. J.* **2000**, *6*, 3069. (i) Kahne, D.; Gut, S.; DePue, R.; Mohamadi, F.; Wanat, R. A.; Collum, D. B.; Clardy, J.; Van Duyne, G. J. *Am. Chem. Soc.* **1984**, *106*, 4865. (j) Reich, H. J.; Sikorski, W. H.; Thompson, J. L.; Sanders, A. W.; Jones, A. C. *Org. Lett.* **2006**, *8*, 4003. (k) Larranaga, O.; de Cozar, A.; Bickelhaupt, F. M.; Zangi, R.; Cossio, F. P. *Chem. - Eur. J.* **2013**, *19*, 13761.
- (27) (a) We found that *R,R*- and *S,S*-1,2-cyclohexanediamines are not equivalent purities. Although the source of the differences was not found, we alleviated the problem by resolving *trans*-cyclohexanediamine, <sup>27b</sup> N-methylating the methyls, <sup>17</sup> recrystallizing the resulting TMCDA as its HCl salt, <sup>17</sup> and evaluating the optical purity by <sup>13</sup>C NMR spectroscopy by adding 2 equiv of (+)-taddol in toluene-*d*<sub>8</sub>. <sup>30c</sup> (b) Larrow, J. F.; Jacobsen, E. N. *Org. Synth.* **1998**, *10*, 96. (c) Seebach, D.; Beck, A. K.; Heckel, A. *Angew. Chem., Int. Ed.* **2001**, *40*, 92.
- (28) Representative studies of TMCDA in organolithium chemistry: (a) Hodgson, D. M.; Stefane, B.; Miles, T. J.; Witherington, J. *J. Org. Chem.* **2006**, *71*, 8510. (b) Cabello, N.; Kizirian, J.-C.; Gille, S.; Alexakis, A.; Bernardinelli, G.; Pinchard, L.; Caille, J.-C. *Eur. J. Org. Chem.* **2005**, *2005*, 4835. (c) Cointeaux, L.; Alexakis, A. *Tetrahedron: Asymmetry* **2005**, *16*, 925. (d) Mealy, M. J.; Luderer, M. R.; Bailey, W. F.; Sommer, M. B. *J. Org. Chem.* **2004**, *69*, 6042. (e) Strohmman, C.; Gessner, V. H. *J. Am. Chem. Soc.* **2007**, *129*, 8952. (f) Strohmman, C.; Gessner, V. H. *J. Am. Chem. Soc.* **2008**, *130*, 11719.
- (29) (a) Niemeyer, J.; Kehr, G.; Fröhlich, R.; Erker, G. *Dalton Trans.* **2009**, 3731. (b) Williard, P. G.; Tata, J. R.; Schlessinger, R. H.; Adams, A. D.; Iwanowicz, E. J. *J. Am. Chem. Soc.* **1988**, *110*, 7901. (c) Jones, C.; Junk, P. C.; Leary, S. G.; Smithies, N. A. *J. Chem. Soc., Dalton Trans.*

2000, 3186. (d) Muller, G.; Brand, J. *Z. Anorg. Allg. Chem.* **2005**, 631, 2820. (e) Rajeswaran, M.; Begley, W. J.; Olson, L. P.; Huo, S. *Polyhedron* **2007**, 26, 3653. (f) Kathirgamanathan, P.; Surendrakumar, S.; Antipan-Lara, J.; Ravichandran, S.; Chan, Y. F.; Arkley, V.; Ganeshamurugan, S.; Kumaravel, M.; Paramswara, G.; Partheepan, A.; Reddy, V. R.; Bailey, D.; Blake, A. J. *J. Mater. Chem.* **2012**, 22, 6104.

(30) (a) Arnett, E. M.; Nichols, M. A.; McPhail, A. T. *J. Am. Chem. Soc.* **1990**, 112, 7059. (b) Graalman, O.; Klingebiel, U.; Clegg, W.; Haase, M.; Sheldrick, G. M. *Angew. Chem., Int. Ed. Engl.* **1984**, 23, 891. (c) Williard, P. G.; Salvino, J. M. *Tetrahedron Lett.* **1985**, 26, 3931. (d) Jastrzebski, J. T. B. H.; van Koten, G.; Christophersen, M. J. N.; Stam, C. H. *J. Organomet. Chem.* **1985**, 292, 319. (e) Strauch, J.; Warren, T. H.; Erker, G.; Frohlich, R.; Saarenketo, P. *Inorg. Chim. Acta* **2000**, 300-302, 810. (f) Driess, M.; Dona, N.; Merz, K. *Chem. - Eur. J.* **2004**, 10, 5971. (g) Dippel, K.; Keweloh, N. K.; Jones, P. G.; Klingebiel, U.; Schmidt, D. Z. *Naturforsch., B: Chem. Sci.* **1987**, 42, 1253. (h) Davies, R. P.; Wheatley, A. E. H.; Rothenberger, A. *J. Organomet. Chem.* **2006**, 691, 3938. (i) Nichols, M. A.; McPhail, A. T.; Arnett, E. M. *J. Am. Chem. Soc.* **1991**, 113, 6222. (j) Davies, J. E.; Davies, R. P.; Dunbar, L.; Raithby, P. R.; Russell, M. G.; Snaith, R.; Warren, S.; Wheatley, A. E. H. *Angew. Chem., Int. Ed. Engl.* **1997**, 36, 2334. (k) Brehon, M.; Cope, E. K.; Mair, F. S.; Nolan, P.; O'Brien, J. E.; Pritchard, R. G.; Wilcock, D. J. *J. Chem. Soc., Dalton Trans.* **1997**, 3421. (l) Schmidt-Base, D.; Klingebiel, U. *Chem. Ber.* **1989**, 122, 815. (m) Armbruster, F.; Armbruster, N.; Klingebiel, U.; Noltemeyer, M.; Schmatz, S. Z. *Naturforsch., B: Chem. Sci.* **2006**, 61, 1261. (n) Apeloig, Y.; Zharov, I.; Bravo-Zhivotovskii, D.; Ovchinnikov, Y.; Struchkov, Y. J. *J. Organomet. Chem.* **1995**, 499, 73. (o) Graser, M.; Kopacka, H.; Wurst, K.; Muller, T.; Bildstein, B. *Inorg. Chim. Acta* **2013**, 401, 38.